



Original Article

Experimental and quantum chemical investigation for the single and competitive adsorption of cationic dyes onto activated carbon

Umar Yunusa^{a,*}, Bishir Usman^a, Muhammad Bashir Ibrahim^a

^aDepartment of Pure and Industrial Chemistry, Bayero University, P.M.B.3011, BUK, Kano-Nigeria.

ARTICLE INFO

Article history:

Received 15 March 2020

Revised 3 January 2021

Accepted 4 January 2021

Keywords:

Adsorption;

Cationic dyes;

Ionic strength;

Binary system;

Quantum chemical parameters.

ABSTRACT

Single and competitive adsorption studies were performed to scrutinize the removal of two cationic dyes, namely, crystal violet (CV) and malachite green (MG) by adsorption onto activated carbon (BAC) derived from *Balanites aegyptiaca* seed shell. The BAC was characterized via scanning electron microscopy (SEM), Fourier transform infrared spectroscopy (FTIR) and pH of point of zero charge (pH_{pzc}) analysis. The physicochemical parameters influencing the adsorption process, namely, pH, contact time, adsorbent weight, initial concentration, temperature and ionic strength were examined. Moreover, Density Functional Theory (DFT) studies were performed to investigate the chemical reactivity of the dye molecules. Experimental results indicated that maximum adsorption of both dyes was achieved at pH 8.0 and equilibrium was attained after contact time of 50 min for MG and 60 min for CV. The competitive adsorption results showed lower adsorption capacities as compared to the single adsorption results indicating antagonistic interaction. Isotherm and kinetic models were employed for fitting the experimental data. The sorption kinetics was found to obey the pseudo second order model. The equilibrium data suggests that Freundlich model could represent the dyes uptake onto the adsorbent. Thermodynamic analysis revealed that the adsorption is a spontaneous and endothermic process. The quantum chemical investigation performed on the tested dyes using DFT method have affirmed that the MG molecules are more reactive ($\Delta E = 1.236$ eV), electrophilic and have the capacity to adsorb strongly on the BAC surface compared to the CV ($\Delta E = 1.476$ eV). The results attested that BAC has great potential for cationic dyes adsorption from aqueous environment.

1. Introduction

The pollution of precious water sources with potentially harmful substances via natural and anthropogenic activities has become a global phenomenon requiring pressing scientific attention. In particular, the indiscriminate release of industrial effluent laden with synthetic dyes into water systems has become an alarming issue in recent years [1]. Synthetic dyes are extensively utilized in various application contexts, such as textiles, cosmetics, leather, pharmaceuticals, food processing, petroleum, rubber and printing [2]. Indeed, large amount of water are used in industrial operations leading to the released of

contaminated water, and specifically dye-bearing wastewater. The synthetic dyes are considered unique among different water pollutants in the sense that they are noticeable to the bare eye even at low concentration [3]. Among all synthetic dyes used by the textile industry, cationic dyes are the brightest class with obvious coloration observed even at concentration as low as 1 ppm [4]. The stable structure and synthetic origin of most dyes confers high photostability and thus making their decolorization and degradation difficult [5]. The existence of these substances in aqueous systems has a major implication;

* Corresponding author.

E-mail address: umaryunusa93@gmail.com; mbibrahim.chm@buk.edu.ng

Peer review under responsibility of University of Echahid Hamma Lakhdar.

2716-9227/© 2021 The Authors. Published by University of Echahid Hamma Lakhdar.. This is an open access article under the CC BY-NC license

(<https://creativecommons.org/licenses/by-nc/4.0/>).

<http://dx.doi.org/10.5281/zenodo.4504565>

their toxicity, carcinogenicity and mutagenicity severely affect human health and the aquatic environment [6]. Therefore, the removal of dyes from effluents is essential to lessen their deleterious impacts on humans and the environment.

To date, several treatment approaches like chemical precipitation, adsorption, membrane filtration, evaporation, reverse osmosis, ion exchange and coagulation have been explored for remediation of wastewater [7]. Among the aforementioned techniques, adsorption has gained prominence in wastewater treatment because of its operative and economic advantages [8]. A wide range of adsorbent materials have been explored for dye removal such as activated carbon [9], nanoparticles [10], layered double hydroxides [11] and polymer composite [12]. Activated carbon is the most prominent adsorbent and has been recognized as one of the best available alternatives in the evacuation of pollutants from wastewater [13]. Due to its distinct properties, activated carbon exhibits extremely high adsorption efficiency for many adsorbates including cationic dyes. However, its large-scale application in wastewater treatment is hampered by its relatively high cost [14]. In the search for low cost adsorbents, intensive efforts have been made in the fabrication of activated carbon from renewable, low-cost and locally available resources like waste materials.

Balanites aegyptiaca seed shell (BASS) is an undesirable lignocellulosic waste, whose disposal has been an issue of concern in recent years [15]. A promising strategy to manage these wastes that is less explored is their utilization as raw material in the preparation of high value-added adsorbents. It was already proved that BASS was efficient adsorbent for removing atrazine from aqueous solution [16]. However, there are only a few published information about the dye adsorption capability of this material [17]. Furthermore, there is no documented report on the use of BASS as adsorbent for the simultaneous adsorption of dyes in multi-adsorbate systems. However, the actual industrial effluents customarily contain more than one kind of pollutant. So it is imperative to examine the simultaneous adsorption of dyes because sole pollutant rarely exist in effluent.

Density functional theory (DFT) has become a powerful and informative theoretical tool for studying the chemical reactivity of organic substances and for describing intermolecular interactions [18,19]. It offers a remarkable level of accuracy and precision compared to other existing approaches. Although DFT-based molecular descriptors have been extensively applied in drug design and corrosion inhibition studies, their usefulness in adsorption studies is gradually being appreciated [20]. Recently, quantum

chemical calculations using DFT are used in adsorption studies to deduce the influence of molecular structure on adsorption efficiency as well as to determine the interactions between the examined adsorbate and the target adsorbent.

The purposes of the present study distributed into five parts were: (i) to prepare activated carbon from BASS using a zinc chloride (ZnCl_2) chemical activation approach; (ii) to characterize the adsorbent using Fourier transform infrared spectroscopy (FTIR), scanning electron microscopy (SEM) and pH at point of zero charge (pH_{pzc}) analysis; (iii) to assess its removal performance for CV and MG from their respective individual and combined aqueous solutions; (iv) to investigate the kinetics, isotherms and thermodynamics of the dye adsorption process (v) to carry out quantum chemical studies of theoretical reactivity of CV and MG molecules using DFT-based descriptors in order to justify the experimental results of the adsorption.

2. Materials and Methods

2.1. Chemicals and Materials

Crystal violet ($\text{C}_{25}\text{H}_{30}\text{N}_3\text{Cl}$, 407.98 g mol⁻¹, CI 42555) and Malachite green ($\text{C}_{23}\text{H}_{25}\text{N}_2\text{Cl}$, 364.92 g mol⁻¹, CI 42000) were procured from E. Merck (Mumbai, India). Analytical grade hydrochloric acid, zinc chloride, sodium hydroxide and sodium nitrate were bought from Sigma-Aldrich. All chemical reagents were utilized as received throughout the adsorption studies. *Balanites aegyptiaca* seed shells were sourced from a local market in Gashua-Yobe, Nigeria. The activated carbon was synthesized with zinc chloride as activating agent using a two-step chemical activation procedure [21]. Briefly, the dried sample was initially subjected to pyrolysis at 700°C in a muffle furnace (SXL-1008) for 90 min. A certain amount of the resulting char was mixed with zinc chloride (ZnCl_2) with the mass ratio set at 2:1 (ZnCl_2 : char). This was followed by further thermal treatment at 750°C and for 90 min. The activated product was subsequently cooled, leached with 250 mL dilute hydrochloric acid and then repeatedly washed with distilled water until the washing solution pH attained a neutral value.

2.2. Characterization Methods

The surface morphology and chemical characteristics of the sample were examined using different analytical techniques including SEM and FTIR. The FTIR spectra of the adsorbent in the range of 4000–600 cm⁻¹ were recorded with FTIR spectrophotometer (Agilent Technologies; Cary 630). SEM images of samples were obtained using scanning electron microscope (PRO: X: Phenom World 800-07334). The images were captured at 10 kv and 1000x

enlargement. With regard to distribution of charges on BAC surface, the pH of zero charge point (pH_{pzc}) of the adsorbent was determined according to the salt addition method reported by Bakatula et al. [22].

2.3. Preparation of Single and Binary Dye Solutions

Stock solutions of CV and MG (1000 mgL^{-1}) were prepared by dissolving 1 g (each) of the respective dyes in 100 mL beaker and made up to 1000 mL in a graduated flask with distilled water. Binary dye solution (CV + MG) was prepared the same way with a mass ratio of 1:1. Experimental solutions of lower concentrations were subsequently prepared from the stock solution by successive dilution. These solutions were used for constructing the calibration curve and for adsorption studies.

2.4. Adsorption Experiments

The experiments were conducted in batch mode by contacting specified dose of adsorbent with 100 mL of dyes solution in Erlenmeyer flasks. These flasks were shaken at 150 rpm at 30°C (room temperature) using incubator shaker (New Brunswick Scientific; Innova 4000). The initial solution pH was adjusted to the desired value using 0.1 M HCl and 0.1 M NaOH. The impact of operating variables such as weight of adsorbent (0.15, 0.25, 0.35, 0.45, 0.55 and 0.65 g), initial dye concentration (50, 100, 150, 200 and 250 mg L^{-1}), contact time (5, 10, 20, 30, 60, 90 and 120 min), pH (3, 4, 5, 6, 7, 8 and 9), ionic strength (0, 0.1, 0.2, 0.3, 0.4 and 0.5 M) and temperature (30 , 40 , 50 and 60°C) were examined in individual experiments. After predecided time interval, the adsorbent was separated via filtration using filter paper (Whatman No. 1). The unadsorbed dye concentration in the filtrate was analyzed using UV-Vis spectrophotometer (Perkin Elmer; Labda 35) at absorption maxima of 590 and 617 nm for CV and MG, respectively. For the binary dye system, the experimental protocol and conditions used were as described for monocomponent dye systems. The experiments were replicated three times and only the average results have been presented. The deviation in the results were about 3%. The uptake amount for each dye at equilibrium, q_e (mgg^{-1}) was computed from the relation:

$$q_e = \left(\frac{C_o - C_e}{m}\right)V \quad (1)$$

where C_o and C_e (mgL^{-1}) represent the initial and final dye concentration, respectively. V (L) represent the dye aqueous solution volume and m (g) is the adsorbent mass.

2.5. Quantum Chemical Studies.

The reactivity of CV and MG was elucidated by DFT

calculations using the materials studio 8.0 software (BIOVIA, Accelrys). The geometrical optimizations of CV and MG structures was performed with the DMol³ module using B3LYP/PWC/DND level of theory to conduct electronic structure calculations. The quantum chemical parameters were obtained from energies associated with the highest occupied molecular orbital (HOMO; E_H), lowest unoccupied molecular orbital (LUMO; E_L), and an energy gap ($\Delta E = E_H - E_L$). The general behavior of CV and MG molecules was analyzed using the global reactivity parameters like chemical potential (μ), chemical hardness (η), chemical softness (σ) and electrophilicity power (ω), which can be linked with the Frontier orbital energies as depicted by the following equations [23]:

$$\mu = \frac{(E_H + E_L)}{2} \quad (2)$$

$$\eta = \frac{(E_L - E_H)}{2} \quad (3)$$

$$\sigma = \frac{1}{\eta} \quad (4)$$

$$\omega = \frac{\mu^2}{2\eta} \quad (5)$$

3. Results and Discussion

3.1. Characterization of the BAC

The SEM is an important technique for examining the surface texture and porosity of the adsorbent material. SEM observation depicted in Fig. 1a illustrated the irregular and porous structure of BAC. However, diminished porous surfaces were visualized after CV and MG adsorption (Figs. 1b and 1c) which signifies the accommodation of the dye molecules in the adsorbent pores. The surface functionalities of the activated carbon as obtained from FTIR are presented in Fig. 2a. The presence of stretching for $-\text{OH}$, aromatic C-H, and $-\text{CSH}$ are indicated by peaks at 3327 , 1447 and 870 cm^{-1} , respectively [24]. However, the spectra after adsorption (Figs. 2b and 2c) revealed appreciable changes in the occurrences or position of some peaks. These changes may be taken as confirmation of some sort of interaction between the dye molecules and the adsorbent surface [25].

3.2. Adsorption Studies

3.2.1. Impact of contact time and adsorption kinetics

Since the adsorption process is time-dependent, it is crucial to investigate the sorption rate in process design. The faster the adsorption rate, the lesser are the operational costs that favor the adsorbent for large-scale application [26]. For, this reason, the impact of contact time of adsorbates with BAC was studied to ascertain the equilibrium time to maximally remove dye molecules and the adsorption kinetics. Fig. 3a illustrates a rise in adsorption capacity in

both individual and binary system with increase in contact time between the adsorbates and adsorbent. This is because more time familiarizes the dye molecules to bond with the adsorbent [27].

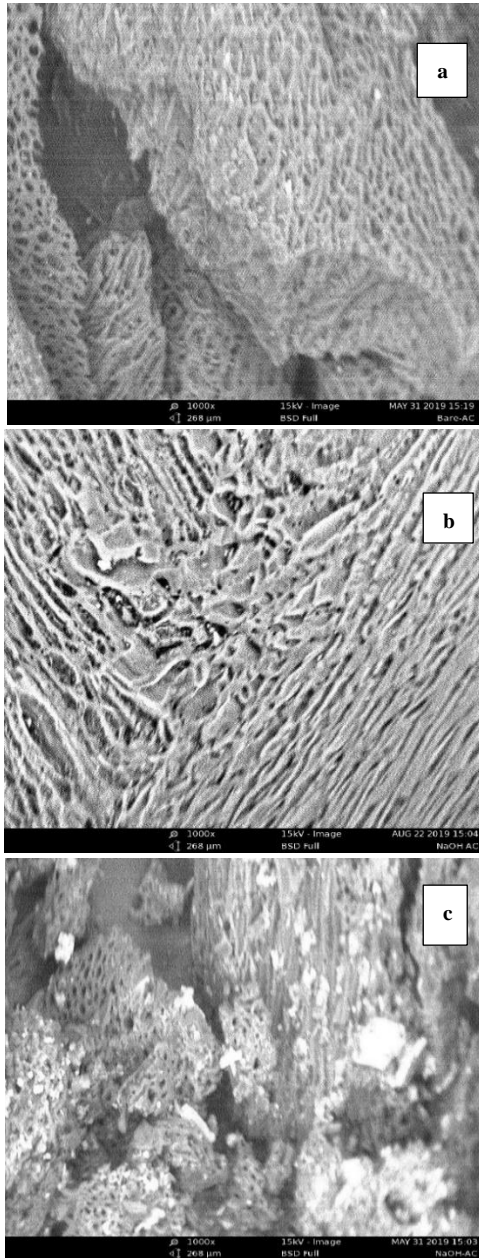


Fig 1. SEM images of BAC (a) before adsorption; (b) after CV adsorption; (c) after MG adsorption.

The graph indicates that the rise in adsorption capacity was insignificant during contact times after 50 minutes in case of MG and 60 minutes in case of CV. Thus, 50 and 60 min contact period were defined as the equilibrium time. Also, the equilibrium time for the respective dyes are the same in both systems. It is clear from Fig 3a that the dyes sorption obey a three step mechanism. During the early rapid

predominant step, large number of sites are vacant and accessible for dyes uptake on the adsorbent. During the later slower step, the movement of dyes into the pores creates repulsion between the dye molecules on the solid and the bulk phases. During the final equilibrium step, the removal process almost ceases due to unavailability of vacant sites on the adsorbent to accommodate the adsorbates [28].

To study the dynamic sorption behavior of the adsorbates on BAC, the pseudo first order [29] and pseudo second order [30] models were employed to simulate the kinetic data and their linear forms are expressed by Eqs. 6 and 7, respectively.

$$\ln(q_e - q_t) = \ln q_e - k_1 t \quad (6)$$

$$\frac{t}{q_t} = \frac{1}{k_2 q_e^2} + \frac{t}{q_e} \quad (7)$$

where, q_t and q_e represent the amount of dyes adsorbed on adsorbent at any instance t and at equilibrium, respectively, k_1 and k_2 are the corresponding rate constants.

In the light of interrelationship coefficient (R^2), the kinetic data fit properly to pseudo second order model (Fig 3b) than pseudo first order (Fig 3c) in all the dye systems and the kinetic parameters were summarized in Table 1. It can be observed in Table 1 that the predicted q_e values are in close agreement with the experimental values for pseudo second order model. The applicability of the pseudo second order model hints chemisorption as the rate controlling step. The rate constant, k_2 , of CV and MG in binary dye systems are lower than those for mono-adsorbate systems which is likely due to antagonistic effect in the adsorption system. The rate constant for MG are higher than those for CV in both single and binary dye systems. The results intimate that the MG adsorption process is faster than CV adsorption in both mono- and binary-dye solutions [31].

3.2.2. Impact of solution pH

CV and MG are cationic dyes that exist in the form of positively charged ions in aqueous medium. Therefore, as ionic species, the extent of their adsorption is basically controlled by the net surface charge on the adsorbent, which in turn is influenced by the solution pH. The influence of solution pH on the dyes uptake is depicted in Fig. 4a. The adsorption capacity was found to increase with the increasing solution pH. The maximal CV and MG uptake in both single and binary systems was observed at pH 8.0. This implies that the basic pH condition favors the sorption of dye ions. This phenomenon can be interpreted in a better way by an adsorbent characteristic known as the pH of point of zero charge (pH_{pzc}).

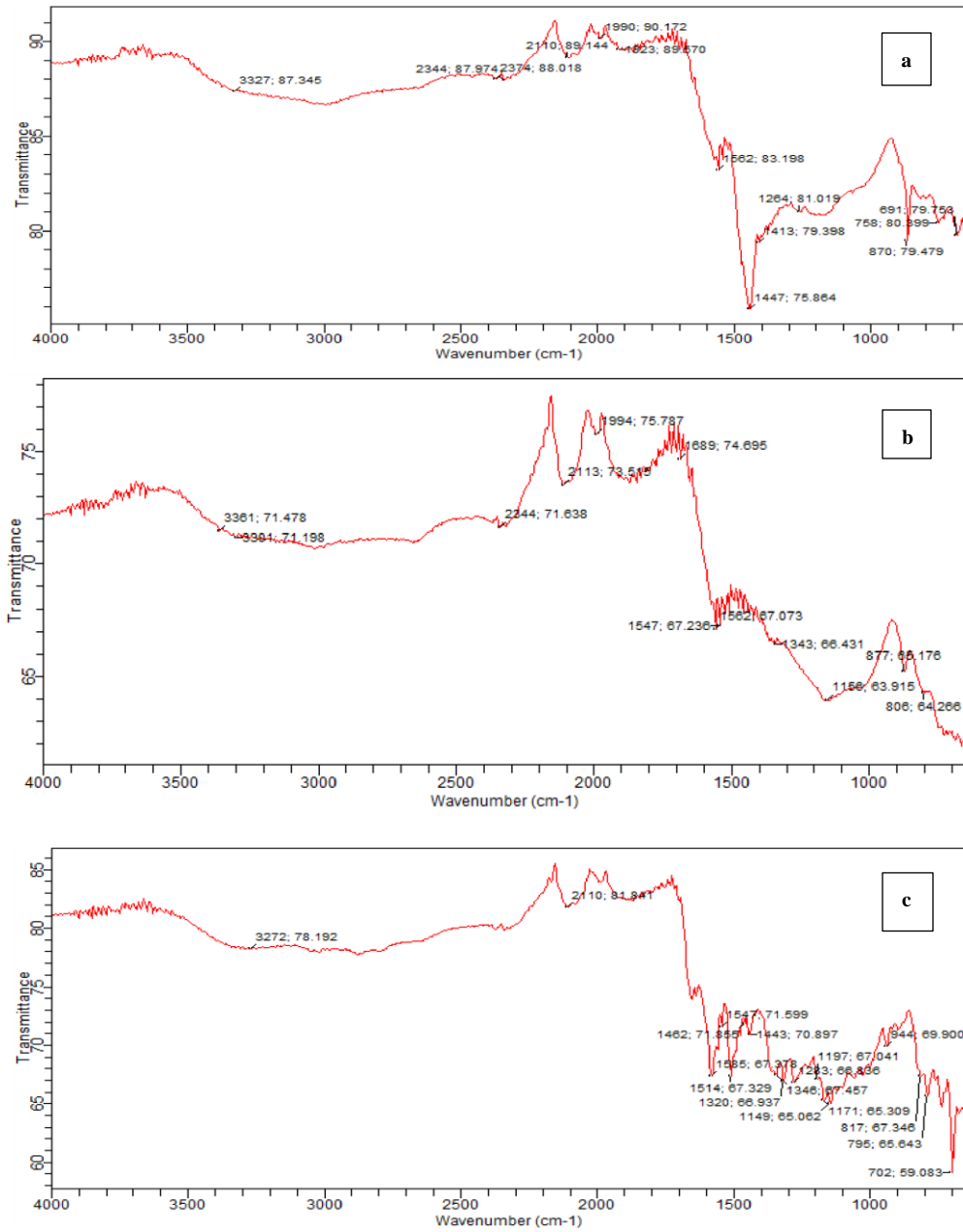


Fig 2. FTIR spectrum of (a) BAC; (b) CV-loaded BAC; (c) MG-loaded BAC

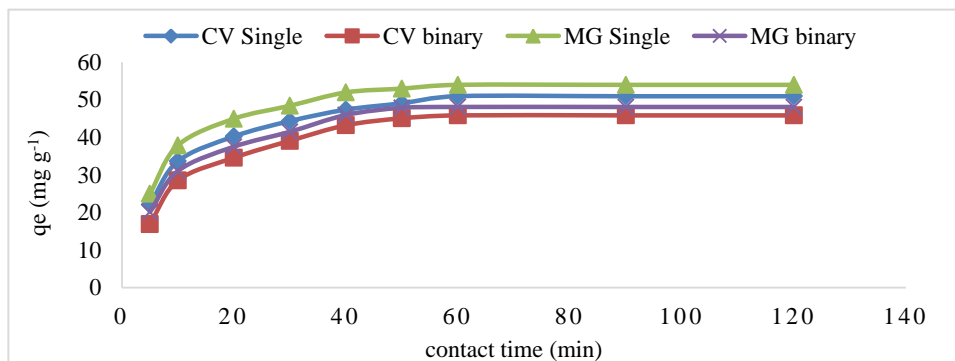


Fig 3a. Impact of contact time on dyes uptake by BAC (Conditions: C₀ = 100 mg L⁻¹, adsorbent weight = 0.15 g, temperature = 30°C).

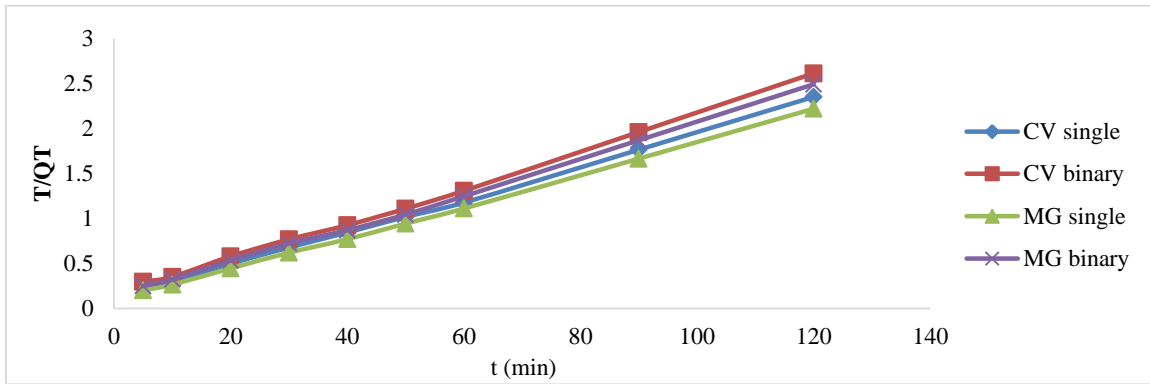


Fig 3b. Pseudo second order kinetic fit for dyes adsorption onto BAC

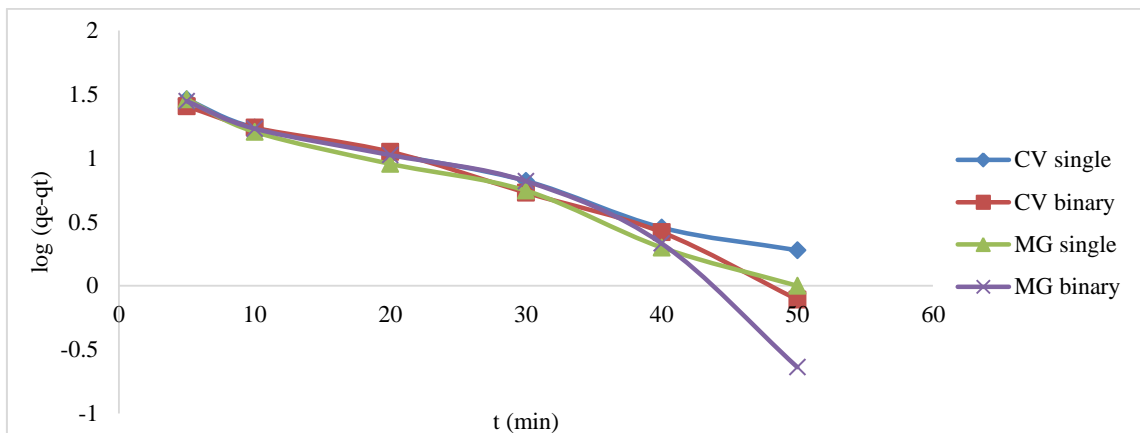


Fig 3c. Pseudo first order kinetic fit for dyes adsorption onto BAC

Table 1. The parameters of different kinetic models for dyes adsorption onto BAC

System	$q_{e,exp}$ (mgg ⁻¹)	Pseudo first order			Pseudo second order		
		$q_{e,cal}$ (mgg ⁻¹)	k_1	R^2	$q_{e,cal}$ (mgg ⁻¹)	$k_2 \times 10^{-3}$	R^2
CV single	50.99	35.62	0.058	0.9897	54.34	2.97	0.9990
CV binary	45.87	40.70	0.075	0.9755	49.50	2.70	0.9976
MG single	54.01	38.91	0.072	0.9890	56.82	3.64	0.9991
MG binary	48.12	59.14	0.095	0.9021	51.54	3.10	0.9981

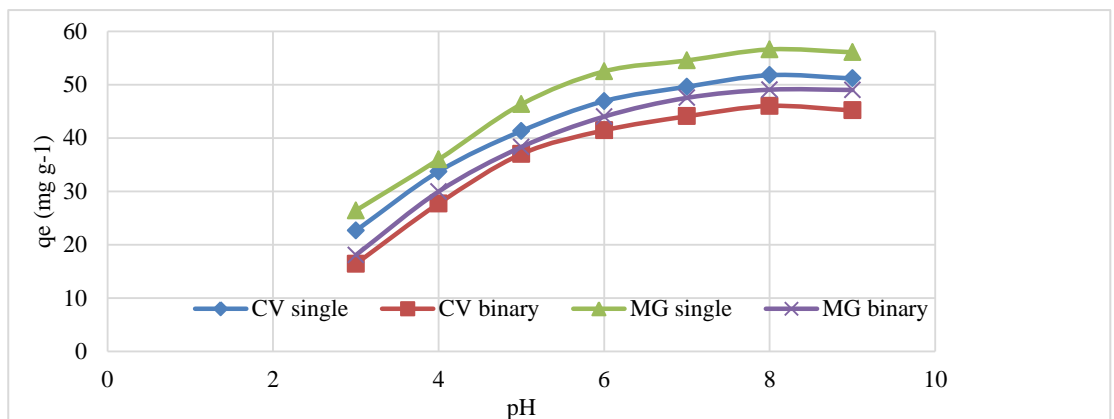


Fig 4a. Impact of solution pH on dyes uptake by BAC (Conditions: $C_o = 100 \text{ mg L}^{-1}$, adsorbent weight = 0.15 g, contact time = 60 min, temperature = 30°C).

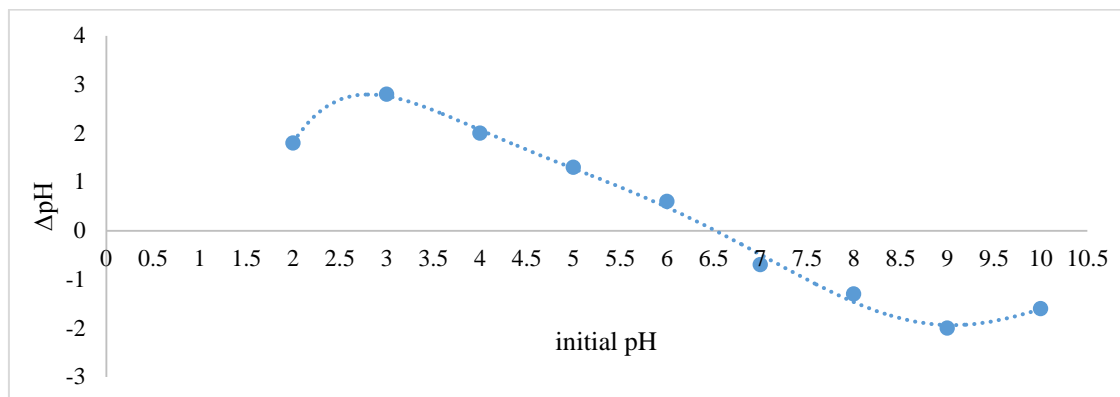


Fig 4b. Determination of pH_{pzc} of BAC

The pH_{pzc} of ACBA was found to be 6.5 (Fig 4b). This value signifies that at $\text{pH} > \text{pH}_{\text{pzc}}$ (6.5), the adsorbent surface becomes deprotonated due to excess hydroxyl ions, thus leading to enhanced affinity between the dye cations and the negatively charged surface of the adsorbent through electrostatic attraction and result in maximum uptake. Conversely at $\text{pH} < \text{pH}_{\text{pzc}}$, relatively low dye sorption has been observed which is majorly attributed to the protonation of the adsorbent surface which hampers the uptake of dye cations due to electrostatic repulsive forces [32]. A similar trend of pH influence was previously reported for the sorption of CV onto wood apple shell carbon [33] and MG onto durian seed carbon [34].

3.2.3. Impact of adsorbent weight

The amount of adsorbent employed in the adsorption process is essential because it dictates the adsorbent-adsorbate ratio in the process and also in cost projection [35]. The variation of the amount of dyes adsorbed with adsorbent weight in both single and binary solutions is presented in Fig 5. Results demonstrated that the adsorption capacity decreased as the adsorbent dose was increased. Similar trend of adsorbent weight effect was reported for the simultaneous adsorption of dye and Pb(II) onto activated carbon [36]. The decline in adsorption capacity with an increase in adsorbent weight implies that available active sites for lower dosages were adequately occupied by sorbate molecules in solution [37].

3.2.4. Impact of ionic strength

The industrial effluents are typically associated with various ionic substances such as inorganic salts. A major limitation resulting from the non-selectivity of adsorbent is that it also interacts with non-target components present in the wastewater. This in turn leads to higher adsorbent dosage demand to achieve the needed maximum adsorption efficiency [38]. Since sodium chloride is frequently used as stimulator in dyeing processes [39], the effect of ionic strength on the removal of CV and MG in mono-

component solution was tested, as shown in Fig 6. The results revealed that the increase in ionic strength of solution causes a decrease in the amount of CV and MG adsorbed onto BAC. However, this decrease reached a plateau at NaCl concentration of 0.3 M. It is worthy of noting that the influence of ionic strength was tested at pH 8.0 where the adsorbent and adsorbates were oppositely charged. The decrease in amount of dyes adsorbed with an increase in salt concentration could be attributed to competition for available active sites between the cationic dye ions and the positively charged $\text{Na}^+_{(\text{aq})}$ being introduced. Furthermore, $\text{Na}^+_{(\text{aq})}$ ions being smaller in size would easily access anionic sites on surface of adsorbent compared to the larger cationic dye ions. These findings are consistent with those reported previously by other researchers for the adsorption of dyes [40,41].

3.2.5. Impact of initial concentration and adsorption isotherms

The initial adsorbate concentration is a significant parameter that influences the diffusion and mass transfer dynamics of the sorption of dyes onto adsorbent. The influence of initial concentration on the sorption capacity of adsorbates is displayed in Fig 7. When Fig 7 is observed, the amount of adsorbed dyes per unit gram of BAC is increased by the increase of the initial concentration of sorbates. This is because the initial sorbate concentration provided the needed driving force to overwhelm mass transfer resistance for dye transport between the aqueous phase and the surface of the BAC. In addition, the increase in initial concentration improves the interaction between the dyes and adsorbent [42].

The adsorption isotherms are crucial for analyzing the interaction of sorbate molecules on the adsorbent surface. In the present study, the isotherm models of Langmuir [43] and Freundlich [44] were utilized to model both the systems and their linear forms are represented by the following equations:

$$\frac{C_e}{q_e} = \frac{1}{K_L q_{\max}} + \frac{C_e}{q_{\max}} \quad (8)$$

$$\log q_e = \log K_f + \frac{1}{n} \log C_e \quad (9)$$

where, q_e (mg g^{-1}) and C_e (mg L^{-1}) represent the dye uptake and concentration at equilibrium, respectively. q_{\max} (mg g^{-1}) and K_L (L mg^{-1}) are Langmuir isotherm constants which express the maximum adsorption capacity and adsorption free energy, respectively. The K_F (L mg^{-1}) and n are Freundlich isothermic constants furnishing information on adsorption capacity and adsorption yield, respectively. The values of characteristics parameters of Freundlich and Langmuir models were summarized in Table 2. By judging the interrelationship coefficients, one can deduce that the Freundlich model matched the experimental data quite well for all the dyes implying that; (a) the BAC surface is heterogeneous; (b) the adsorption sites on BAC are not energetically equivalent; (c) the adsorbed dye molecules are organized as a multilayer and; (d) there are interactions between adsorbed dye molecules. It is worth noting that removal of CV by waste active sludge [45] and MG by banana peel [46] have also been found to obey Freundlich isotherm. The Freundlich constant, n , gives information about the favorability of the process. When the value of $n > 1$ or $n < 1$, this signifies that the adsorption is linked to a favorable physical or chemical process, respectively. The value of n in all the systems is > 1 , indicating a convenient physical adsorption.

3.2.6. Impact of temperature and adsorption thermodynamics

Temperature is an important parameter influencing adsorption. It was observed that the amount of dyes adsorbed increased as the temperature was raised (Fig. 8a). This might probably be due variations in the activation energies of the adsorbent active sites. Hence, at a low temperature, only the active sites with low activation energy participated in adsorption, while those with higher activation energy might participate only at elevated temperatures. Another reason for the improved adsorption at higher temperature is the increase in kinetic energy of the sorbate molecules which enhance their collision frequency and mobility within the pores of the adsorbent [47]. Similar phenomenon was also observed for adsorption of CV by clay [48] and MG by activated carbon [49].

Standard changes in enthalpy (ΔH°), entropy (ΔS°) and Gibbs free energy (ΔG°) are important thermodynamic parameters that must be investigated for proper assessment of the nature of any adsorption process. These parameters were calculated to provide insights regarding the spontaneity, thermal character and favorability of the

sorption. The following equations were used to evaluate their values under the experimental conditions employed:

$$\Delta G^\circ = \Delta H^\circ - T\Delta S^\circ \quad (10)$$

$$\Delta G^\circ = -RT \ln K_c \quad (11)$$

$$K_c = \frac{C_{\text{ADS}}}{C_e} \quad (12)$$

Where, C_{ADS} and C_e (mg dm^{-3}) represent the equilibrium concentration of dyes on the adsorbent and in the liquid phase, respectively, K_c is the equilibrium constant of adsorption, R is the gas constant ($8.314 \text{ J K}^{-1} \text{ mol}^{-1}$) and T is the temperature (K). Eq. 6 was used to obtain the values of ΔG° at different temperatures.

The plot of ΔG° against T displayed in Fig. 8b was used for the evaluation of magnitude of ΔS° and ΔH° . The estimated values of ΔG° , ΔH° , and ΔS° for adsorption of dyes by BAC are listed in Table 3. The values of ΔG° were negative signifying the spontaneity and thermodynamic favorability of the sorption process. In addition, the degree of spontaneity of the process was observed to increase with increasing temperature. The ΔG for physisorption and chemisorption processes are in the range of -20 to 0 kJ mol^{-1} and -80 to 400 kJ mol^{-1} , respectively [50]. ΔG values obtained in this study are within the range of -20 to 0 kJ mol^{-1} , implying that the adsorption of the sorbates onto the surface of the BAC occurred primarily through a physisorption mechanism. The positive value of ΔH° reflects the endothermicity of the process. The positive value of ΔS° was a reflection of high affinity of the BAC for the dyes. Similar trend in thermodynamics has also been reported for the adsorption of CV onto bambusa tulda [51] and MG onto malt bagasse [52].

3.2.7. Co-adsorption behavior of dyes

The adsorption of dyes in binary solution was studied to gain insight about the impact presented by one sorbate to another when they coexist in a medium. Fig 9 illustrates the relationship between residual and initial dye concentrations. From the plot, it is clear that the residual dyes concentration in the binary solutions are higher than in single systems probably due to competitive effect of the co-adsorbate for the available adsorption sites. This implies that the presence of one sorbate in solution suppresses to an extent the adsorption of the other. The effect of CV presence on MG or vice versa can also be examined using relative adsorption capacity expressed as [53]:

$$q^r = \frac{q_{m,i}}{q_{s,i}} \quad (13)$$

where $q_{m,i}$ and $q_{s,i}$ represent the adsorption capacity of adsorbate i in the binary and single dye systems with the

same operating condition, respectively.

From Eq. 13, the following deductions can be made; (a) antagonistic interaction occurred when the adsorption capacity of an adsorbent is suppressed in a solution containing other components ($q^r < 1$), (b) synergistic interaction occurred when the adsorption capacity of an adsorbent is improved in a solution containing other components ($q^r > 1$), and (c) there is non-interaction if the adsorption capacity of an adsorbent is independent of the presence or absence of co-adsorbate in solution ($q^r = 1$) [54]. The experimental results indicate that the relative adsorption capacities (q^r) for both CV and MG are < 1 indicating that there was inhibitive interference of one component on the other during adsorption (antagonistic effect). Similar antagonistic trends were reported in the binary solutions of basic yellow and maxilon red [55], remazol brilliant blue and disperse orange [56], and basic blue and basic yellow [57].

3.2.8. Selectivity analysis for binary system

Selectivity analysis was performed to investigate the adsorbent preference towards a particular component in the binary solution. Usually the selectivity factor (α) is utilized to ascertain the molecular selectivity and affinity of adsorbent and is defined as follows [58]:

$$\alpha \left(\frac{MG}{CV} \right) = \frac{q_{MG,b}}{q_{CV,b}} \quad (14)$$

where, $q_{MG,b}$ and $q_{CV,b}$ represent adsorption capacity of the MG and CV in the binary component system, respectively. The value of $\alpha_{(MG/CV)}$ being greater than unity signifies that the adsorbent has more affinity towards MG than CV [59]. According to experimental results, $\alpha_{(MG/CV)}$ is greater than unity indicating preferential adsorption of MG onto the BAC as compared to CV. The factors that influence the preference of adsorbent for different types of adsorbates may be linked to the characteristics of the active sites (functional groups, structure and surface properties), the solution chemistry (pH and ionic strength) and the properties of the adsorbates (molecular structure, molecular weight, concentration, solubility and ionic nature) [60]. The higher affinity of BAC towards MG can be explained by its lower solubility (3 g L^{-1}) compared with CV (16 g L^{-1}). In addition, the lower molecular weight of MG enables it to diffuse faster into the pores of the adsorbent than CV. This hints that porosity played vital role in the adsorption process. Similar phenomenon was reported for the preference of Thiourea-modified polymer adsorbent towards methylene blue dye compared to MG in a binary system [61]. This outcome will be further justified by the following quantum chemical study.

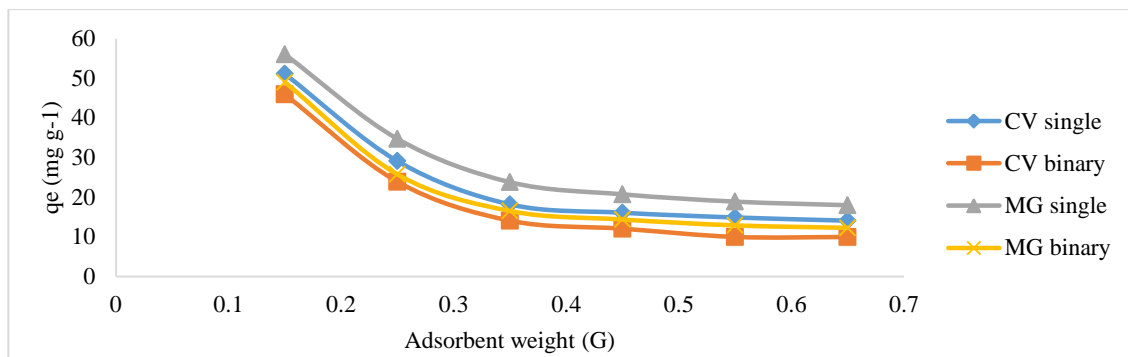


Fig 5. Impact of adsorbent weight on dyes uptake by BAC (Conditions: $C_o = 100 \text{ mg L}^{-1}$, contact time = 60 min, pH = 8.0, temperature = 30°C).

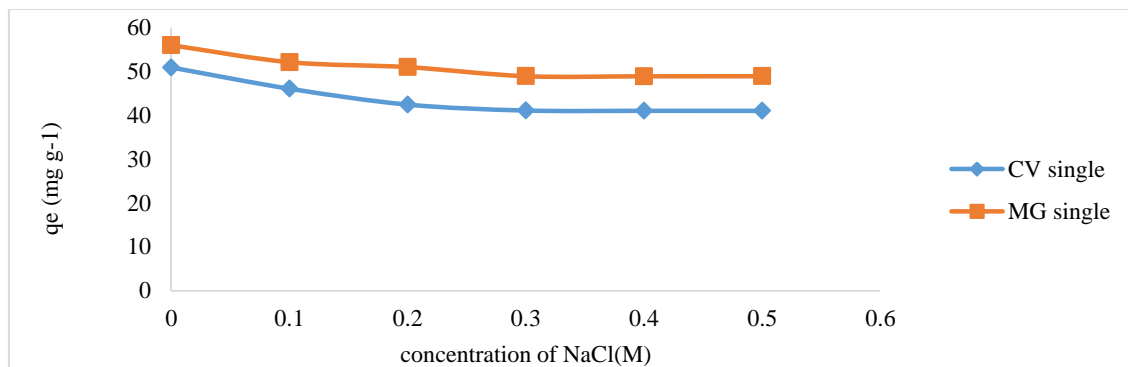


Fig 6. Impact of ionic strength on dyes uptake by BAC (Conditions: $C_o = 100 \text{ mg L}^{-1}$, contact time = 60 min, pH = 8.0, temperature = 30°C).

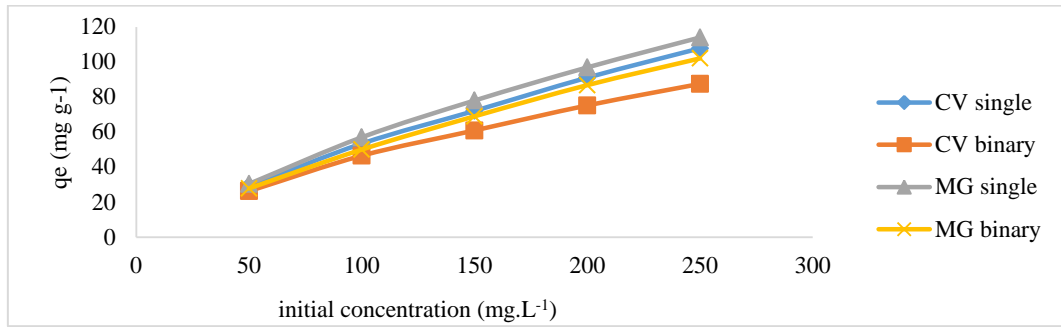


Fig 7. Impact of initial concentration on dyes uptake by BAC (contact time = 60 min, pH = 8.0, adsorbent weight = 0.15 g, temperature = 30°C).

Table 2. The parameters of different isotherm models for dyes adsorption onto BAC

Isotherm	parameters	CV single	CV binary	MG single	MG binary
Langmuir	q_{max} (mg g ⁻¹)	138.88	113.64	140.85	136.98
	K_L (L mg ⁻¹)	0.03	0.02	0.02	0.05
	R_L	0.24	0.30	0.29	0.20
	R^2	0.9698	0.9771	0.9709	0.9817
Freundlich	K_F (L mg ⁻¹)	11.55	8.29	16.11	9.07
	n	2.00	2.02	2.22	1.88
	R^2	0.9974	0.9978	0.9956	0.9999

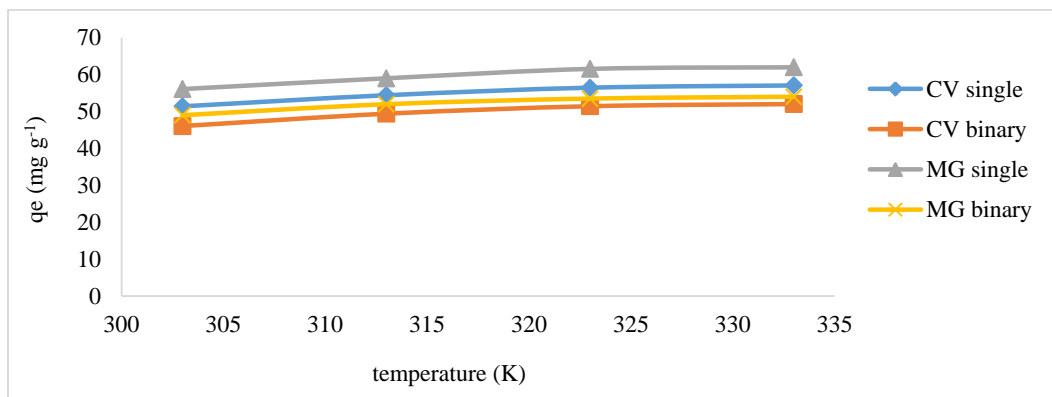


Fig 8a. Impact of temperature on dyes uptake by BAC (Conditions: $C_o = 100 \text{ mg L}^{-1}$, contact time = 60 min, pH = 8.0, adsorbent dose = 0.15 g).

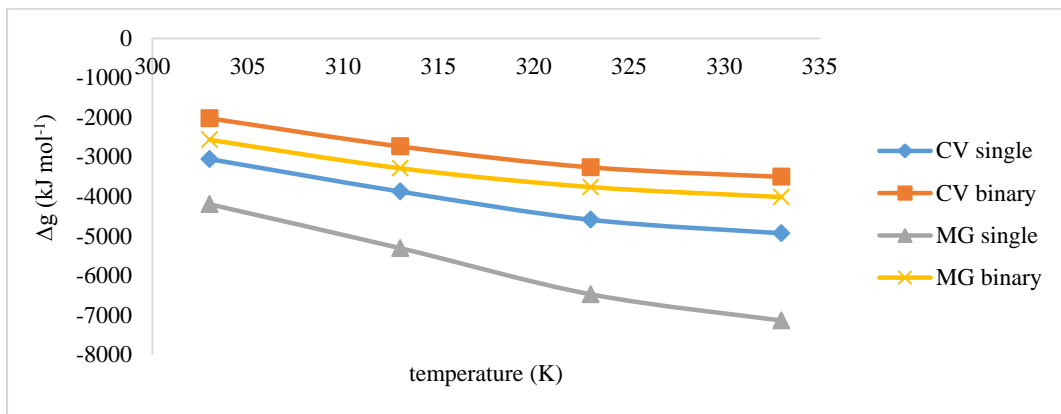


Fig 8b. Gibbs plot for estimation of thermodynamic parameters

Table 3. The thermodynamic parameters for dyes adsorption onto BAC

System	ΔH (kJ mol ⁻¹)	ΔS (kJ mol ⁻¹ K ⁻¹)	ΔG (kJ mol ⁻¹)			
			303K	313K	323K	333K
CV single	16.03	0.063	-3.055	-3.876	-4.590	-4.929
CV binary	12.92	0.050	-2.024	-2.735	-3.265	-3.504
MG single	25.97	0.099	-4.197	-5.307	-6.674	-7.136
MG binary	11.92	0.048	-2.566	-3.286	-3.762	-4.014

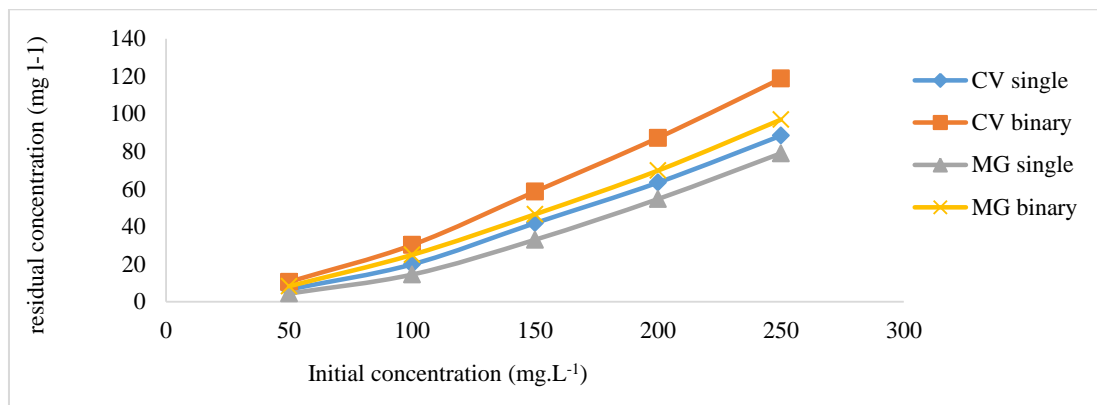


Fig 9. Variation of initial with residual dyes concentrations

3.3. Quantum Chemical Studies

In the current work, the quantum chemical computations using DFT were performed to examine the influence of the molecular structure on the adsorption of CV and MG onto the BAC surface. The optimized geometries, electron density, HOMO and LUMO orbitals of the dye molecules are exposed in Fig. 10. Molecular orbitals play a vital role in the understanding of reactivity at the atomic level. It can be seen from Figs. 10b and 10c that both HOMO and LUMO orbitals are widely spread on the area of both the sorbate molecules. Thus, both dyes have a high electron-attracting capacity signifying their cationic nature [62].

The computed energies of orbitals and energy gap E_H , E_L , and ΔE in addition to chemical potential (μ), global hardness (η), global softness (σ), electrophilicity power (ω), surface area (SA) and surface volume (SV) data of the tested CV and MG dyes are displayed in Table 4. As reported, the E_H is basically associated to the capacity of a molecule to donate electrons, while the E_L reflects the ability of the molecule to capture electrons. Consequently, a low value of ΔE designates a high reactivity of a molecule. The values of energy gap (ΔE) computed for studied molecules are CV ($\Delta E = 1.476$ eV), and MG ($\Delta E = 1.236$ eV). The results signify that MG is more reactive because of the low energy gap value [63]. The reactivity and stability of dye molecules can be assessed by the values of global hardness and softness. Generally, lower

values of global hardness (η) and higher values of global softness (σ) of molecules can promote their adsorption to a surface [64]. The CV molecule ($\eta = 0.738$ eV) has a high hardness value relative to MG ($\eta = 0.618$ eV). The electrophilicity power (ω) depicts the ability of molecules to gain electrons. The value of ω for CV ($\omega = 4.086$ eV) is lower than MG ($\omega = 6.016$ eV) which hints that CV is weak electrophile when compared with MG, consequently the MG dye will be adsorbed first in a binary system [65]. A reactive electrophile is exemplified by high values of electrophilicity index (ω) and chemical potential (μ) [66]. The values μ for the molecules are MG ($\mu = 2.727$ eV) and CV ($\mu = 2.454$ eV). Thus, MG has a higher value of μ and ω compared to CV, accordingly, the MG molecule is more reactive electrophile than CV. Better adsorption of MG dye than CV dye on BAC is also favored by lower values of surface area (SA) and surface volume (SV). The lower the surface volume and area of the adsorbate, the more easily it will compete to fit into the adsorption matrix of the adsorbent [67]. According to theoretical results from computed quantum descriptors, MG molecule present high reactivity, softness and electrophilicity compared to CV molecules. These outcomes are in concurrence with adsorption experiments and proved the experimental results associated to the high uptake of MG by BAC compared to CV.

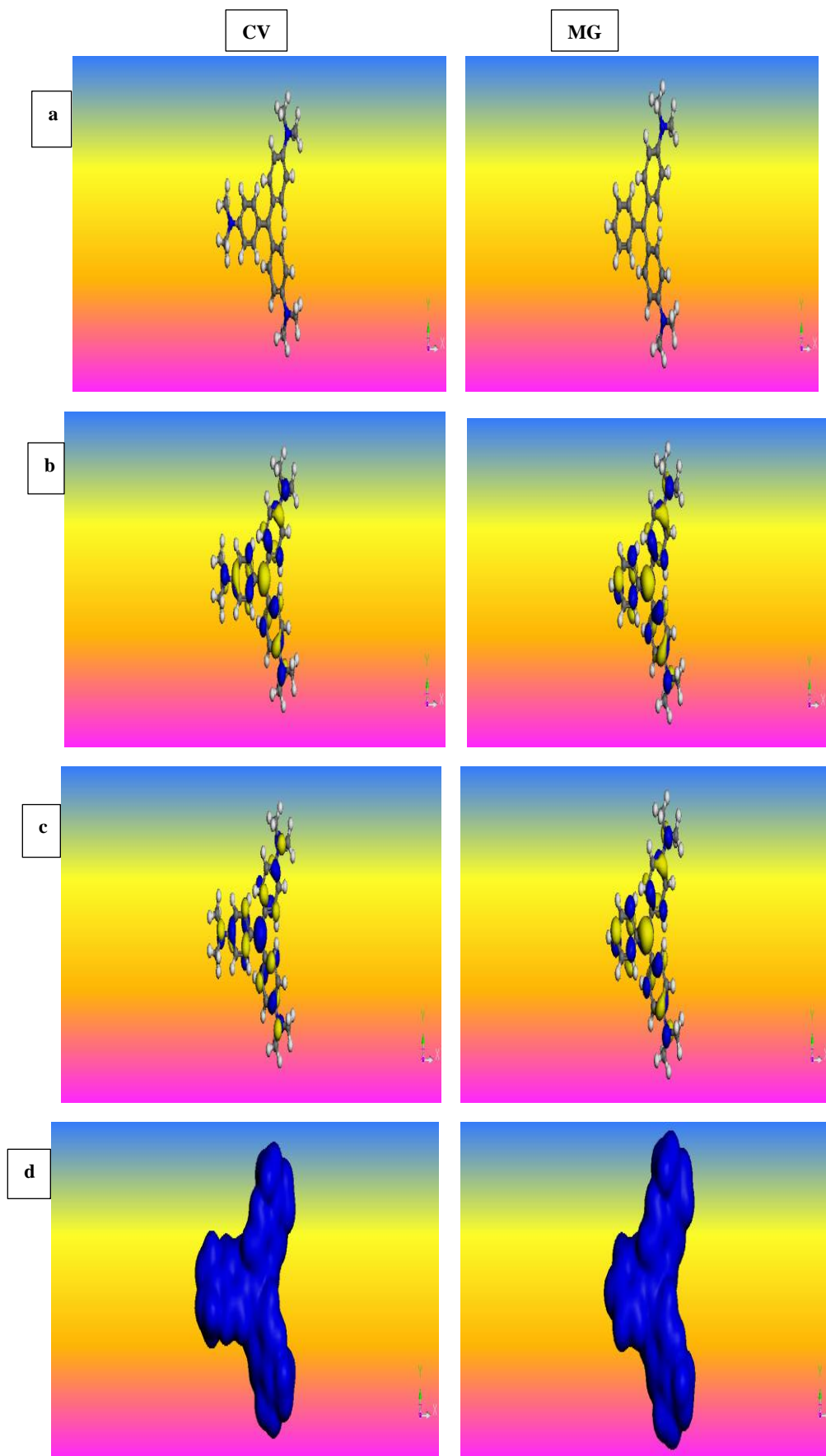


Fig 10. (a) optimized geometry; (b) HOMO; (c) LUMO; (d) electron density of the dyes using DFT

Table 4. Computed quantum chemical parameters for CV and MG dyes using B3LYP/PWC/DND level of theory

Descriptor	CV	MG
E_H (eV)	-3.192	-3.345
E_L (eV)	-1.716	-2.109
ΔE (eV)	1.476	1.236
η (eV)	0.738	0.618
σ (eV)	1.355	1.618
ω (eV)	4.086	6.016
μ (eV)	2.454	2.727
SA (\AA^2)	446.346	397.008
SV (\AA^3)	480.781	428.011

4. Conclusion

The adsorption of CV and MG onto BAC in single and binary systems was scrutinized. The optimum conditions for maximum dyes uptake were pH: 8.0, adsorbent weight: 0.15 g, contact time: 60 min and temperature: 333K. The

sorption kinetics was found to obey the pseudo second order model. The equilibrium data suggests that Freundlich model could represent the dyes uptake onto the adsorbent. Thermodynamic analysis revealed that the adsorption is a spontaneous and endothermic process. Relative adsorption capacity for the binary system indicated antagonistic adsorption. The quantum chemical studies of the reactivity of the tested dyes are in good agreement with the experimental observations. Overall, the results affirmed the suitability of BAC as alternative adsorbent for cationic dyes removal from aqueous medium.

Acknowledgements

Umar Yunusa extend his sincere appreciation to Dr. Ayuba Abdullahi Muhammad, Bayero University Kano, for the installation of materials studio 8.0 software (BIOVIA, Accelrys).

References

- Sabna V, Thampi SG, Chandrakaran S. Adsorption of crystal violet onto functionalised multi-walled carbon nanotubes: equilibrium and kinetic studies. *Ecotoxicology and Environmental Safety*. 2016;134:390-397.
- Raval NP, Shah PU, Shah NK. Malachite green “a cationic dye” and its removal from aqueous solution by adsorption. *Applied Water Science*. 2017;7(7):3407-3445.
- Mashkoor F, Nasar A, Asiri AM. Exploring the reusability of synthetically contaminated wastewater containing crystal violet dye using tectona grandis sawdust as a very low-cost adsorbent. *Scientific reports*. 2018;8(1):1-6.
- Mao J, Won SW, Min J, Yun YS. Removal of Basic Blue 3 from aqueous solution by *Corynebacterium glutamicum* biomass: Biosorption and precipitation mechanisms. *Korean Journal of Chemical Engineering*. 2008;25(5):1060-1064.
- Forgacs E, Cserhati T, Oros G. Removal of synthetic dyes from wastewaters: a review. *Environment international*. 2004;30(7):953-971.
- Li W, Ma Q, Bai Y, Xu D, Wu M, Ma H. Facile fabrication of gelatin/bentonite composite beads for tunable removal of anionic and cationic dyes. *Chemical Engineering Research and Design*. 2018;134:336-346.
- Wang Y, Yang R, Li M, Zhao Z. Hydrothermal preparation of highly porous carbon spheres from hemp (*Cannabis sativa* L.) stem hemicellulose for use in energy-related applications. *Industrial Crops and Products*. 2015;65:216-226.
- Xiong W, Zeng Z, Li X, Zeng G, Xiao R, Yang Z, Zhou Y, Zhang C, Cheng M, Hu L, Zhou C. Multi-walled carbon nanotube/amino-functionalized MIL-53 (Fe) composites: remarkable adsorptive removal of antibiotics from aqueous solutions. *Chemosphere*. 2018;210:1061-1069.
- Ahmad MA, Afandi NS, Adegoke KA, Bello OS. Optimization and batch studies on adsorption of malachite green dye using rambutan seed activated carbon. *Desalination and Water treatment*. 2016;57(45):21487-21511.
- Ali I, Peng C, Khan ZM, Sultan M, Naz I, Ali M, Farid HU, Mahmood MH, Ahsen R. Removal of Crystal Violet and Eriochrome Black T Dye from Aqueous Solution by Magnetic Nanoparticles Biosynthesized from Leaf Extract of *Fraxinus Chinensis* Roxb. *Pol. J. Environ. Stud.* 2019;28(4):2027-2040.
- Shan RR, Yan LG, Yang YM, Yang K, Yu SJ, Yu HQ, Zhu BC, Du B. Highly efficient removal of three red dyes by adsorption onto Mg–Al-layered double hydroxide. *Journal of Industrial and Engineering Chemistry*. 2015;21:561-568.
- Fabryanty R, Valencia C, Soetaredjo FE, Putro JN, Santoso SP, Kurniawan A, Ju YH, Ismadji S. Removal of crystal violet dye by adsorption using bentonite–alginate composite. *Journal of Environmental Chemical Engineering*. 2017;5(6):5677-5687.
- Derbyshire F, Jagtoyen M, Andrews R, Rao A, Martin-Gullon I, Grulke EA. Carbon materials in environmental applications. *Chemistry and physics of carbon*. 2001:1-66.
- Netzahuatl-Muñoz AR, del Carmen Cristiani-Urbina M, Cristiani-Urbina E. Chromium biosorption from Cr (VI) aqueous solutions by *Cupressus lusitanica* bark: Kinetics, equilibrium and thermodynamic studies. *PLoS One*. 2015;10(9):e0137086.
- Yunusa U, Ibrahim MB. Reclamation of malachite green-bearing wastewater using desert date seed shell: adsorption isotherms, desorption and reusability studies. *Chemsearch Journal*. 2019;10(2):112-122.
- Giwa SO, Moses JS, Adeyi AA, Giwa A. Adsorption of atrazine from aqueous solution using desert date seed shell activated carbon. *Journal of Engineering Research and Development*. 2018;1(3):317-325.
- Yunusa U, Bishir U, Ibrahim MB. Kinetic and thermodynamic studies of malachite green adsorption using activated carbon prepared from desert date seed shell. *Algerian Journal of Engineering and Technology*. 2020;2:37-45.

18. Sharma S, Duggal V, Srivastava AK, Mehra R. Assessment of radiation dose from exposure to radon in drinking water from Western Haryana, India. *International Journal of Environmental Research*. 2017;11(2):141-147.
19. El Kassimi A, Boutouil A, El Himri M, Laamari MR, El Haddad M. Selective and competitive removal of three basic dyes from single, binary and ternary systems in aqueous solutions: A combined experimental and theoretical study. *Journal of Saudi Chemical Society*. 2020;24(7):527-544.
20. Rotaru I, Varvara S, Gaina L, Muresan LM. Theoretical, thermodynamic and electrochemical analysis of biotin drug as impending corrosion inhibitor for mild steel in 15% hydrochloric acid. *Appl. Surf. Sci.* 2014;321:188-196.
21. Wang X, Wang S, Yin X, Chen J, Zhu L. Activated carbon preparation from cassava residue using a two-step KOH activation: preparation, micropore structure and adsorption capacity. *Journal of Biobased Materials and Bioenergy*. 2014;8(1):35-42.
22. Bakatula EN, Richard D, Neculita CM, Zagury GJ. Determination of point of zero charge of natural organic materials. *Environmental Science and Pollution Research*. 2018;25(8):7823-7833.
23. Ouasfi N, Zbair M, Bouzikri S, Anfar Z, Bensitel M, Ahsaine HA, Sabbar E, Khamliche L. Selected pharmaceuticals removal using algae derived porous carbon: experimental, modeling and DFT theoretical insights. *RSC advances*. 2019;9(17):9792-9808.
24. Ali I, Peng C, Ye T, Naz I. Sorption of cationic malachite green dye on phyto-genic magnetic nanoparticles functionalized by 3-mercaptopropanoic acid. *RSC advances*. 2018;8(16):8878-8897.
25. Giwa AA, Oladipo MA, Abdulsalam KA. Adsorption of Rhodamine B from single, binary and ternary dye systems using sawdust of *Parkia biglobosa* as adsorbent: isotherm, kinetics and thermodynamics studies. *Journal of Chemical and Pharmaceutical Research*. 2015;7(2):454-475.
26. Istratie R, Stoia M, Păcurariu C, Locovei C. Single and simultaneous adsorption of methyl orange and phenol onto magnetic iron oxide/carbon nanocomposites. *Arabian Journal of Chemistry*. 2019;12(8):3704-3722.
27. Mahaninia MH, Rahimian P, Kaghazchi T. Modified activated carbons with amino groups and their copper adsorption properties in aqueous solution. *Chinese Journal of Chemical Engineering*. 2015;23(1):50-56.
28. Mokkaapati RP, Mokkaapati J, Ratnakaram VN. Kinetic, isotherm and thermodynamics investigation on adsorption of divalent copper using agro-waste biomaterials, *Musa acuminata*, *Casuarina equisetifolia* L. and *Sorghum bicolor*. *Polish Journal of Chemical Technology*. 2016;18(2):68-77.
29. Lagergren SK. About the theory of so-called adsorption of soluble substances. *Sven. Vetenskapsakad. Handlingar*. 1898;24:1-39.
30. Ho YS, McKay G. Pseudo-second order model for sorption processes. *Process biochemistry*. 1999;34(5):451-65.
31. Luo X, Zhang Z, Zhou P, Liu Y, Ma G, Lei Z. Synergic adsorption of acid blue 80 and heavy metal ions (Cu²⁺/Ni²⁺) onto activated carbon and its mechanisms. *Journal of Industrial and Engineering Chemistry*. 2015;27:164-74.
32. Banerjee S, Sharma GC, Gautam RK, Chattopadhyaya MC, Upadhyay SN, Sharma YC. Removal of Malachite Green, a hazardous dye from aqueous solutions using *Avena sativa* (oat) hull as a potential adsorbent. *Journal of Molecular Liquids*. 2016;213:162-172.
33. Doke KM, Yusufi M, Joseph RD, Khan EM. Comparative adsorption of crystal violet and congo red onto ZnCl₂ activated carbon. *Journal of Dispersion Science and Technology*. 2016;37(11):1671-1681.
34. Ahmad MA, Ahmad N, Bello OS. Adsorptive removal of malachite green dye using durian seed-based activated carbon. *Water, Air, & Soil Pollution*. 2014;225(8):1-8.
35. Wanyonyi WC, Onyari JM, Shiundu PM. Adsorption of Congo red dye from aqueous solutions using roots of *Eichhornia crassipes*: kinetic and equilibrium studies. *Energy Procedia*. 2014;50:862-869.
36. Inam EI, Etim UJ, Akpabio EG, Umoren SA. Simultaneous adsorption of lead (II) and 3, 7-Bis (dimethylamino)-phenothiazin-5-ium chloride from aqueous solution by activated carbon prepared from plantain peels. *Desalination and Water Treatment*. 2016;57(14):6540-6553.
37. Cheruiyot GK, Wanyonyi WC, Kiplimo JJ, Maina EN. Adsorption of toxic crystal violet dye using coffee husks: equilibrium, kinetics and thermodynamics study. *Scientific African*. 2019;5:e00116.
38. Mahmoodi NM. Synthesis of core-shell magnetic adsorbent nanoparticle and selectivity analysis for binary system dye removal. *Journal of Industrial and Engineering Chemistry*. 2014;20(4):2050-2058.
39. Ma J, Yu F, Zhou L, Jin L, Yang M, Luan J, Tang Y, Fan H, Yuan Z, Chen J. Enhanced adsorptive removal of methyl orange and methylene blue from aqueous solution by alkali-activated multiwalled carbon nanotubes. *ACS applied materials & interfaces*. 2012;4(11):5749-5760.
40. Shee A, Onyari JM, Wabomba JN, Munga D. Methylene blue adsorption onto coconut husks/poly lactide blended films: equilibrium and kinetic studies. *Chem Mater Res*. 2014;6:28-38.
41. Chieng HI, Lim LB, Priyantha N. Enhancing adsorption capacity of toxic malachite green dye through chemically modified breadnut peel: equilibrium, thermodynamics, kinetics and regeneration studies. *Environmental technology*. 2015;36(1):86-97.
42. Duran C, Ozdes D, Gundogdu A, Senturk HB. Kinetics and isotherm analysis of basic dyes adsorption onto almond shell (*Prunus dulcis*) as a low cost adsorbent. *Journal of Chemical & Engineering Data*. 2011;56(5):2136-2147.
43. Langmuir I. The constitution and fundamental properties of solids and liquids. Part I. Solids. *Journal of the American chemical society*. 1916;38(11):2221-2295.
44. Freundlich H. Über die adsorption in lösungen. *Zeitschrift für physikalische Chemie*. 1907;57(1):385-470.
45. Sahbaz DA, Dandil S, Acikgoz C. Removal of crystal violet dye by a novel adsorbent derived from waste active sludge used in wastewater treatment. *Water Quality Research Journal*. 2019;54(4):299-308.
46. Saechiam S, Sripongpun G. Adsorption of malachite green from synthetic wastewater using banana peel adsorbents. *Songklanakarinn Journal of Science & Technology*. 2019;41(1):21-29.
47. Prasanthi MR, Jayasravanthi M, Nadh RV. Kinetic, thermodynamic and equilibrium studies on removal of hexavalent chromium from aqueous solutions using agro-waste biomaterials, *casuarina equisetifolia* L. and *sorghum bicolor*. *Korean Journal of Chemical Engineering*. 2016;33(8):2374-2383.

48. Collins ON, Elijah OC. ADSORPTION OF A DYE (CRYSTAL VIOLET) ON AN ACID MODIFIED NON-CONVENTIONAL ADSORBENT. *Journal of Chemical Technology & Metallurgy*. 2019;54(1):95-110.
49. Ahmad MA, Afandi NS, Adegoke KA, Bello OS. Optimization and batch studies on adsorption of malachite green dye using rambutan seed activated carbon. *Desalination and Water treatment*. 2016;57(45):21487-21511.
50. Dallel R, Kesraoui A, Seffen M. Biosorption of cationic dye onto "Phragmites australis" fibers: Characterization and mechanism. *Journal of environmental chemical engineering*. 2018;6(6):7247-7256.
51. Laskar N, Kumar U. Adsorption of crystal violet from wastewater by modified bambusa tulda. *KSCE Journal of Civil Engineering*. 2018;22(8):2755-2763.
52. Reis HC, Cossolin AS, Santos BA, Castro KC, Pereira GM, Silva VC, Sousa PT, Dall'Oglio EL, Vasconcelos LG, Morais EB. Malt bagasse waste as biosorbent for malachite green: an ecofriendly approach for dye removal from aqueous solution. *International Journal of Biotechnology and Bioengineering*. 2018;12(4):118-126.
53. Chen B, Yue W, Zhao H, Long F, Cao Y, Pan X. Simultaneous capture of methyl orange and chromium (VI) from complex wastewater using polyethylenimine cation decorated magnetic carbon nanotubes as a recyclable adsorbent. *RSC advances*. 2019;9(9):4722-4734.
54. Wang F, Pan Y, Cai P, Guo T, Xiao H. Single and binary adsorption of heavy metal ions from aqueous solutions using sugarcane cellulose-based adsorbent. *Bioresource technology*. 2017;241:482-490.
55. Chan LS, Cheung WH, Allen SJ, McKay GJ. Equilibrium adsorption isotherm study of binary basic dyes on to bamboo derived activated carbon. *HKIE transactions*. 2017;24(4):182-192.
56. Mavinkattimath RG, Kodialbail VS, Govindan S. Simultaneous adsorption of Remazol brilliant blue and Disperse orange dyes on red mud and isotherms for the mixed dye system. *Environmental Science and Pollution Research*. 2017;24(23):18912-18925.
57. Regti A, El Kassimi A, Laamari MR, El Haddad M. Competitive adsorption and optimization of binary mixture of textile dyes: A factorial design analysis. *Journal of the Association of Arab Universities for Basic and Applied Sciences*. 2017;24:1-9.
58. Tovar-Gómez R, del Rosario Moreno-Virgen M, Moreno-Pérez J, Bonilla-Petriciolet A, Hernández-Montoya V, Durán-Valle CJ. Analysis of synergistic and antagonistic adsorption of heavy metals and acid blue 25 on activated carbon from ternary systems. *Chemical Engineering Research and Design*. 2015;93:755-772.
59. Girish CR. Simultaneous adsorption of pollutants onto the adsorbent review of interaction mechanism between the pollutants and the adsorbent. *Int. J. Eng. Technol*. 2018;7:3613-3622.
60. Singh N, Balomajumder C. Biosorption of Phenol and Cyanide from Synthetic/Simulated Wastewater by Sugarcane Bagasse—Equilibrium Isotherm and Kinetic Analyses. *Water Conservation Science and Engineering*. 2017;2(1):1-4.
61. Adeyi AA, Jamil SN, Abdullah LC, Choong TS, Lau KL, Abdullah M. Simultaneous adsorption of cationic dyes from binary solutions by Thiourea-Modified Poly (acrylonitrile-co-acrylic acid): detailed isotherm and kinetic studies. *Materials*. 2019;12(18):2903.
62. El Haouti R, Ouachtak H, El Guerdaoui A, Amedlous A, Amaterz E, Haounati R, Addi AA, Akbal F, El Alem N, Taha ML. Cationic dyes adsorption by Na-Montmorillonite Nano Clay: Experimental study combined with a theoretical investigation using DFT-based descriptors and molecular dynamics simulations. *Journal of Molecular Liquids*. 2019;290:111139.
63. Regti A, El Ayouchia HB, Laamari MR, Stiriba SE, Anane H, El Haddad M. Experimental and theoretical study using DFT method for the competitive adsorption of two cationic dyes from wastewaters. *Applied Surface Science*. 2016;390:311-9.
64. Guediri A, Bouguettoucha A, Chebli D, Chafai N, Amrane A. Molecular dynamic simulation and DFT computational studies on the adsorption performances of methylene blue in aqueous solutions by orange peel-modified phosphoric acid. *Journal of Molecular Structure*. 2020;1202:127290.
65. Suganthi S, Balu P, Sathyanarayanamoorthi V, Kannappan V, Kamil MM, Kumar R. Structural analysis and investigation of molecular properties of Cefpodoxime acid, a third generation antibiotic. *Journal of Molecular Structure*. 2016;1108:1-5.
66. de Souza TN, de Carvalho SM, Vieira MG, da Silva MG, Brasil DD. Adsorption of basic dyes onto activated carbon: experimental and theoretical investigation of chemical reactivity of basic dyes using DFT-based descriptors. *Applied Surface Science*. 2018;448:662-670.
67. Odoemelam SA, Emeh UN, Eddy NO. Experimental and computational chemistry studies on the removal of methylene blue and malachite green dyes from aqueous solution by neem (*Azadirachta indica*) leaves. *Journal of Taibah University for Science*. 2018;12(3):255-265.

Recommended Citation

Yunusa U, Usman B, Ibrahim MB. Experimental and quantum chemical investigation for the single and competitive adsorption of cationic dyes onto activated carbon. *Alg. J. Eng. Tech*. 2021, 4:7-21. <http://dx.doi.org/10.5281/zenodo.4504565>



This work is licensed under a [Creative Commons Attribution-NonCommercial 4.0 International License](https://creativecommons.org/licenses/by-nc/4.0/)